Molecular Crystals and Liquid Crystals
Publication details, including instructions for authors and subscription information:
http://www.tandfonline.com/loi/gmcl16

Alignment Effects on the Dynamic Scattering Characteristics of an Ester Liquid Crystal

M. J. Little [a], H. S. Lim [a] & J. D. Margerum [a]
[a] Hughes Research Laboratories., Malibu, California, 90265

To cite this article: M. J. Little, H. S. Lim & J. D. Margerum (1977): Alignment Effects on the Dynamic Scattering Characteristics of an Ester Liquid Crystal, Molecular Crystals and Liquid Crystals, 38:1, 207-217

To link to this article: http://dx.doi.org/10.1080/15421407708084387

Mol. Cryst. Liq. Cryst., 1977, Vol. 38, pp. 207–217

Printed in Holland

Alignment Effects on the Dynamic Scattering Characteristics of an Ester Liquid Crystal†

M. J. LITTLE, H. S. LIM and J. D. MARGERUM
Hughes Research Laboratories, Malibu, California 90265

(*Received October 19, 1976*)

The effects of surface alignment are studied on the ac dynamic scattering characteristics of a phenyl benzoate nematic liquid crystal. Seven different alignment modes are used with identical liquid crystal samples by pretreating the conductive glass surfaces to obtain the desired alignments. We find that the threshold voltage (V_{th}) increases with increasing initial average tilt angle ($\bar{\theta}$) between the liquid crystal director and the two electrode surfaces. The V_{th} increases linearly as the $\cos\bar{\theta}$ decreases. The surface-perpendicular alignment ($\bar{\theta} = 90°$) has almost twice the V_{th} of the surface-parallel alignment. The dynamic scattering decay times are considerably shorter when $\bar{\theta} = 0°$ than when $\bar{\theta} > 0°$. The scattering versus voltage curves and the microscopic domain patterns are highly dependent upon the initial alignment, even at 1.5 to 2.0 times V_{th}.

INTRODUCTION

The dynamic scattering[1] of nematic liquid crystals has been studied extensively because of applications in electro-optic displays for electronic calculators, watches, message boards, and even flat panel television.[2] The display characteristics of the dynamic scattering are known to depend on the properties of liquid crystals such as viscosity,[3–6] conductivity,[3,4,7,8] conductivity anisotropy,[9] and dopants.[9,12–15] The dynamic scattering also depends on the electrode spacing[16] and on the surface alignment of the liquid crystals at the electrode. The effect of the alignment on the threshold voltage of domain formation has been predicted from theoretical calculations for two surface orientation conditions.[17–19] Although the importance of surface alignment has been recognized, systematic studies on the effect of

---

† Presented at the Sixth International Liquid Crystal Conference, Kent, Ohio, August 1976.

various alignments have been lacking. In this report we compare the effects of seven different surface alignment modes on the ac dynamic scattering characteristics of a phenyl benzoate liquid crystal which contains conductivity dopants but has no surface alignment dopants.

EXPERIMENTAL

The nematic liquid crystal used in this study is a four-component[12,13] mixture of phenyl benzoates (designated as HRL-2N10) which has a nematic range of about 20° to 55°, and a negative dielectric anisotropy of $\Delta\varepsilon = (5.14 - 5.26) = -0.12$ (25°, 500 Hz). It has a resistivity 10^{11} ohm-cm before adding the conductivity dopants, which were either tetrabutylammonium trifluoromethanesulfonate (TBATMS), or a 1 : 1 (by weight) mixture of di-*n*-butylferrocene (DBF) and (2,4,7-trinitro-9-fluorenylidene)malononitrile (TFM). TBATMS is a salt prepared[20] by reaction of trifluoromethanesulfonic acid and tetrabutylammonium bromide. It is purified by recrystallization from water and drying. DBF and TFM are a redox dopant pair[12,13] in which DBF is an electron donor and TFM is an electron acceptor. Commercial DBF and TFM were purified by vacuum distillation and recrystallization from acetonitrile, respectively. The liquid crystal is doped with 0.1% TBATMS ($\rho_\perp \cong 2.0 \times 10^8$ ohm-cm and $\sigma_\parallel/\sigma_\perp \cong 1.23$) or with 0.5% each of DBF and TFM ($\rho_\perp \cong 1.8 \times 10^9$ and $\sigma_\parallel/\sigma_\perp \cong 1.34$), giving roughly comparable ranges of threshold voltage for the two samples.

Prior to alignment treatments, the indium tin oxide (ITO) conductive glass electrodes (PPG Industries) were cleaned by a sequence of scrubbing, degreasing and chromic acid etch followed by rinsing and drying. Surface-parallel alignment was obtained either by rubbing the electrode surface with Kimwipes or by a 30° angle deposit of about 100 Å of SiO on the electrode surface.[21] A tilted parallel alignment (36° off the surface) was obtained by a 5° angle SiO deposit.[22] The liquid crystal tilt angle ($\bar{\theta}$) was measured by a technique similar to one reported recently,[23] in which we used a differential capacitance measurement. The perpendicular alignment was made by bonding long alkyl chains onto an electrode surface coated with a thin layer of SiO_2. Various alignment modes in test cells (see Figure 1) were obtained by combinations of electrodes with these three basic alignment. The average tilt angle ($\bar{\theta}$) in these cells is assumed to be the average of the two surface angles measured independently in the basic alignment configurations. The electrode spacing of the cells was nominally 13 μm.

The dynamic scattering was measured in transmission, using unpolarized green light (centered at 525 nm) at normal incidence and a silicon photodiode detector with a 2° field of view. The scattering versus voltage curves are from slow-scan measurements with 100 Hz (sinusoidal) signals. Repeti-

CODE (NAME)	DIAGRAM	SURFACE ALIGNMENT	ALIGNMENT TECHNIQUE	TILT ANGLES	$\bar{\theta}$
A (PARALLEL)		//	RUBBING	0°	0°
		//	RUBBING	0°	
B (PARALLEL)	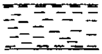	//	30° - SiO	0°	0°
		//	30° - SiO	0°	
C (TWISTED PARALLEL)	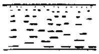	90° //	RUBBING	0°	0°
		//	RUBBING	0°	
D (TWISTED PARALLEL)	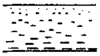	90° //	30° - SiO	0°	0°
		//	30° - SiO	0°	
E TILTED	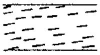	TILTED	5° - SiO	36°	36°
		TILTED	5° - SiO	36°	
F (TWISTED TILTED)		90° TWIST-TILTED	5° - SiO	36°	36°
		TILTED	5° - SiO	36°	
G (SPLAY)		⊥	CHEMICAL	90°	45°
		//	30° - SiO	0°	
H (TILTED SPLAY)		⊥	CHEMICAL	90°	63°
		TILTED	5° - SiO	36°	
I (PERPENDICULAR)		⊥	CHEMICAL	90°	90°
		⊥	CHEMICAL	90°	

FIGURE 1 Alignment modes of the liquid crystal in the test cells.

tive electrical pulses of two seconds on and ten seconds off were used to measure response times, which are defined as follows: delay time is the time between the application of signal and 10% scattering; rise time is the time to go from 10% to 90% scattering; decay time is the time between removal of this signal and return to 10% scattering. The microscopic pictures of the scattering were taken using a Zeiss standard WL polarizing microscope with one polarizer. The polarization direction was adjusted to be parallel to the direction of the surface-parallel component of liquid crystal alignment at the incident electrode surface.

RESULTS AND DISCUSSION

Scattering versus voltage curves

Light transmission as a function of applied voltage (100 Hz) was obtained for cells with each of the nine alignment configurations illustrated in Figure 1. Typical scattering curves (where % scattering = 100 − % transmission) are shown in Figure 2 for the TBATMS salt dopant and in Figure 3 for the DBF/TFM redox dopant system. The dynamic scattering threshold voltage (V_{th}) is obtained by extrapolating the steep rise in scattering back to zero. It agrees, within experimental error, with the threshold voltages observed with the microscope for formation of hydrodynamic domains. The threshold is strongly dependent on the initial surface alignment and V_{th} increases sharply as the average surface tilt angle ($\bar{\theta}$) increases, as discussed below. There appears to be no substantial effect of the 90° twist on the V_{th} values. The scattering curves for parallel or tilted alignment, without a twist, (curves A, B, and E) show a wide voltage range in which the scattering increases steadily with applied voltage above the initial rise near V_{th}. In a display device this type of response can be used to obtain a good gray scale range of scattering intensity. The scattering curves with large average tilt angles such as the surface-perpendicular or splay alignments (curves G, H, and I) show a field realignment effect[24] below the scattering threshold. They go to high scattering levels just above threshold and have a much narrower range of increased scattering at higher voltages. This shows that cells with large

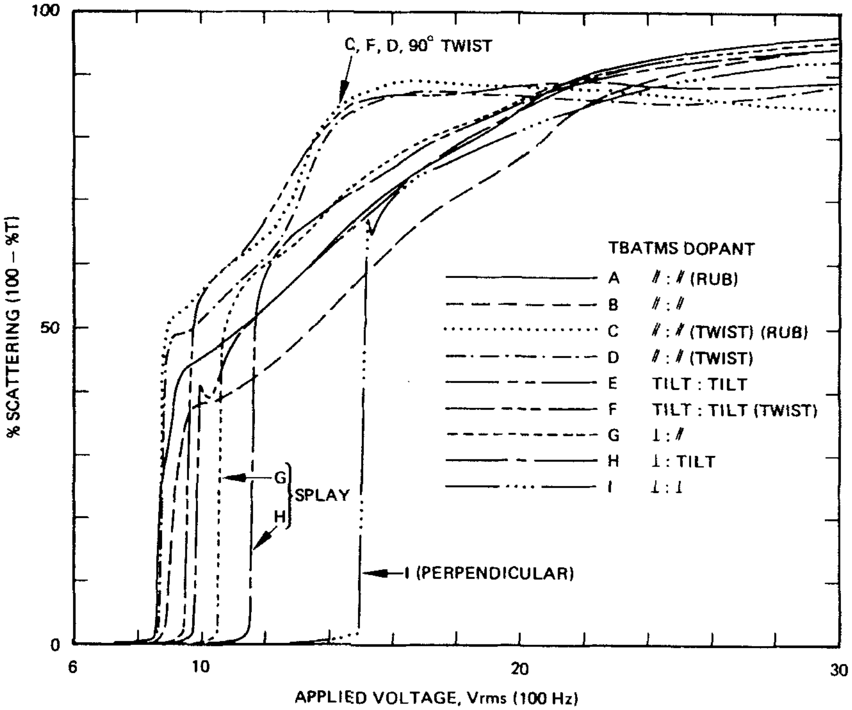

FIGURE 2 Scattering vs voltage curves with various alignments. Dopant: 0.1 % TBATMS Resistivity: $\sim 2 \times 10^8$ Ω-cm. 13 μm thick cells.

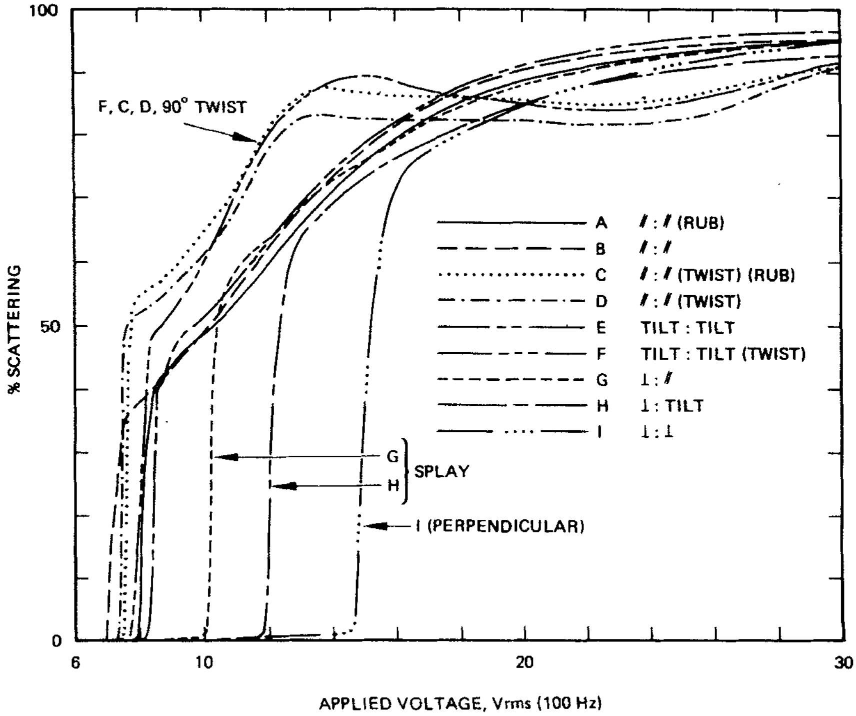

FIGURE 3 Scattering vs voltage curves with various alignments. Dopant: 0.5% each of DBF and TFM. Resistivity: ~ 1.8×10^9 Ω-cm. 13 μm thick cells.

tilt angles are more suitable for two-level displays, with a multiplexed input signal. The twisted nematic cells (curves C, D, and F) show unique type of scattering curve in which a maximum scattering level is reached prior to $2V_{\mathrm{th}}$ and then the scattering level decreases slightly with increasing applied voltage. On the basis of microscope pictures (discussed below), this appears to be related to the strong tendency of the twisted cells to maintain regular hydrodynamic flow patterns at high voltages instead of going into a more random dynamic scattering mode.

Effect of tilt angle on threshold voltage

Duplicate threshold measurements were made on each of two or more cells for each of the nine configurations and average V_{th} values were obtained for each dopant system. These values are given in Figure 4, in which it is shown that V_{th} increases linearly as $\cos \theta$ goes from 1.0 (surface-parallel) to zero (surface-perpendicular). The $\cos \bar{\theta}$ is a factor that is proportional to the

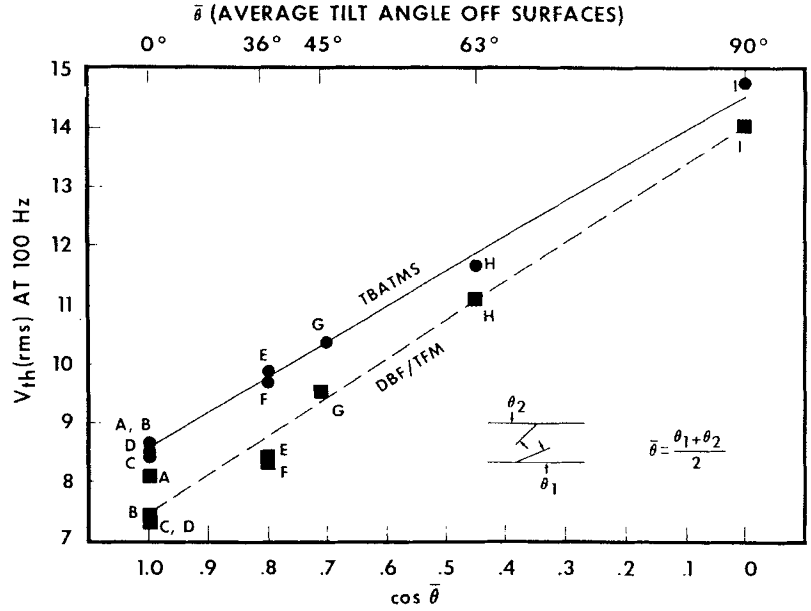

FIGURE 4 Effect of surface tilt angle on the threshold voltage of dynamic scattering.
● : 0.1 % TBATMS, $(\sigma_{\parallel}/\sigma_{\perp}) = 1.23$
■ : 0.5 % each of DBF and TFM, $(\sigma_{\parallel}/\sigma_{\perp}) = 1.34$

average surface-parallel component of length of a liquid crystal molecule, i.e., it is proportional to the projected length of the molecule on the cell surface. The straight line relationship between V_{th} and $\cos \bar{\theta}$ is shown for each dopant in Figure 4. The DBF/TFM dopant system has lower V_{th} values due to its higher conductivity anisotropy in this liquid crystal.[9] We have observed, qualitatively, similar V_{th} vs $\cos \bar{\theta}$ relationships for two other liquid crystals that have more negative values of dielectric anisotropy, but the effect on V_{th} is smaller in magnitude as their $\Delta\varepsilon$ becomes more negative. In the present ester liquid crystal, where $\Delta\varepsilon = -0.12$, the ratio of thresholds for the surface-perpendicular and surface-parallel alignments, $(V_{\text{th}}^{S-\perp}/V_{\text{th}}^{S-\parallel})$, is about 1.7. Another ester liquid crystal with $\Delta\varepsilon = -0.26$ shows the threshold ratio of ~ 1.3. N-*p*-(Methoxybenzylidene)-*p*-*n*-butylaniline (MBBA), whose $\Delta\varepsilon = -0.53$, shows the threshold ratio of only ~ 1.1. Nevertheless, the V_{th} for dynamic scattering appears to be partially dependent upon the magnitude of the surface-parallel component of the initial liquid crystal alignment. Although field alignment of the liquid crystals in surface-perpendicular cells begins far below the scattering threshold, even MBBA is not fully realigned to a surface-parallel condition at the V_{th} for scattering.[25] Only the center part of the cell at V_{th} has an alignment that is nearly parallel to the surface, and there is a tilted alignment region between the center part of the cell and the perpendicular alignment at each surface. The increase of V_{th} with the initial surface tilt ($\bar{\theta}$) is probably because the conductivity anisotropy is less effective in producing turbulence when the liquid crystal is partly tilted in the direction of the applied field, than when the liquid crystal is perpendicular to it. This is also consistent with observations that dynamic scattering in positive dielectric anisotropy materials occurs with surface–parallel but not with surface–perpendicular alignment.[26,27]

The critical frequencies (i.e., dynamic scattering cut-off frequency) of these liquid crystal samples are high enough so that theoretically[28] our ac thresholds would be the same as dc thresholds in the TBATMS-doped samples and only slightly higher than dc values for the DBF/TFM samples. (Experimentally, the dc dynamic scattering thresholds are in fact substantially lower due to charge injection effects.[12,13]) Theoretical calculations[17–19] on the effect of the tilt angle ($\bar{\theta}$) on the dc threshold voltage for hydrodynamic motion have been made considering only the surface–parallel ($\bar{\theta} = 0°$) and the surface–perpendicular ($\bar{\theta} = 90°$) cases. These calculations predict that the surface–perpendicular alignment has a lower V_{th} than the surface–parallel alignment for liquid crystals such as MBBA and *p*-azoxyanisole. Calculations[18] using the Helfrich equations for MBBA predict that $(V_{\text{th}}^{S-\perp}/V_{\text{th}}^{S-\parallel}) = 0.86$. The two-dimensional model of Penz and Ford[19] predicts $V_{\text{th}}^{S-\parallel}$ more accurately for MBBA, but not $V_{\text{th}}^{S-\perp}$, resulting in a predicted $V_{\text{th}}^{S-\perp}/V_{\text{th}}^{S-\parallel}$ of less than 0.7. As noted above, we find that MBBA shows a $(V_{\text{th}}^{S-\perp}/V_{\text{th}}^{S-\parallel}) \cong 1.1$. Our results regarding this ratio are similar to recent results of Barnik *et al.*,[29] who report that a MBBA-like material has $(V_{\text{th}}^{S-\perp}/V_{\text{th}}^{S-\parallel}) \approx 1.4$, and that the ratio increases with less negative values of $\Delta\varepsilon$. It should also be noted that Gruler[18] used the Helfrich equations to predict that $V_{\text{th}}^{S-\perp}/V_{\text{th}}^{S-\parallel}$ ratios > 1 for MBBA-like liquid crystals of small negative dielectric anisotropy, e.g., he calculated a ratio of ~ 1.4 for a liquid crystal with $\Delta\varepsilon = -0.12$, while we find a ratio of ~ 1.7 for our ester.

Response times

Response time measurements were made on the same sets of duplicate cells used for the tilt angle measurements. The average values are shown in Figure 5 for the two dopant systems. Note that a logarithmic time scale is used to compress the data for a graphic format. The actual thickness of each cell was not measured and there are probably enough variations from the nominal 13 μm cell thickness to cause some inaccuracies in the relative response times, which are approximately proportional to the square of the thickness. The decay times are approximately the same for all the cells with surface–parallel alignment ($\bar{\theta} = 0°$ in modes A, B, C, and D) with or

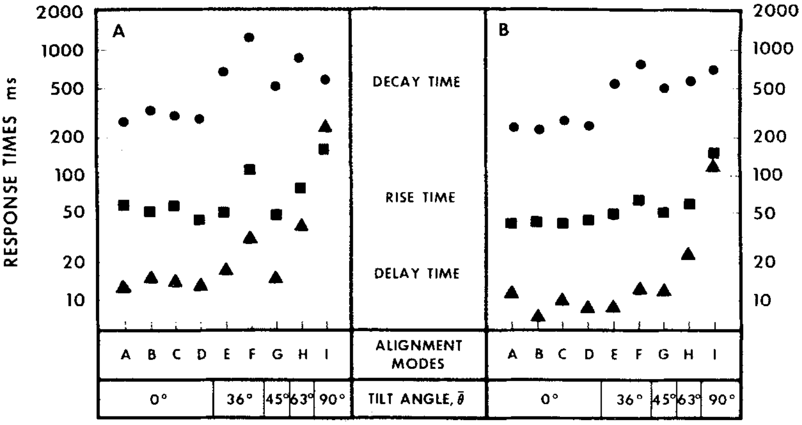

FIGURE 5 Response times of the test cells with various alignments. Nominal electrode separation: 12.7 μm. A: 0.1% TBATMS. B: 0.5% each of DBF and TFM.

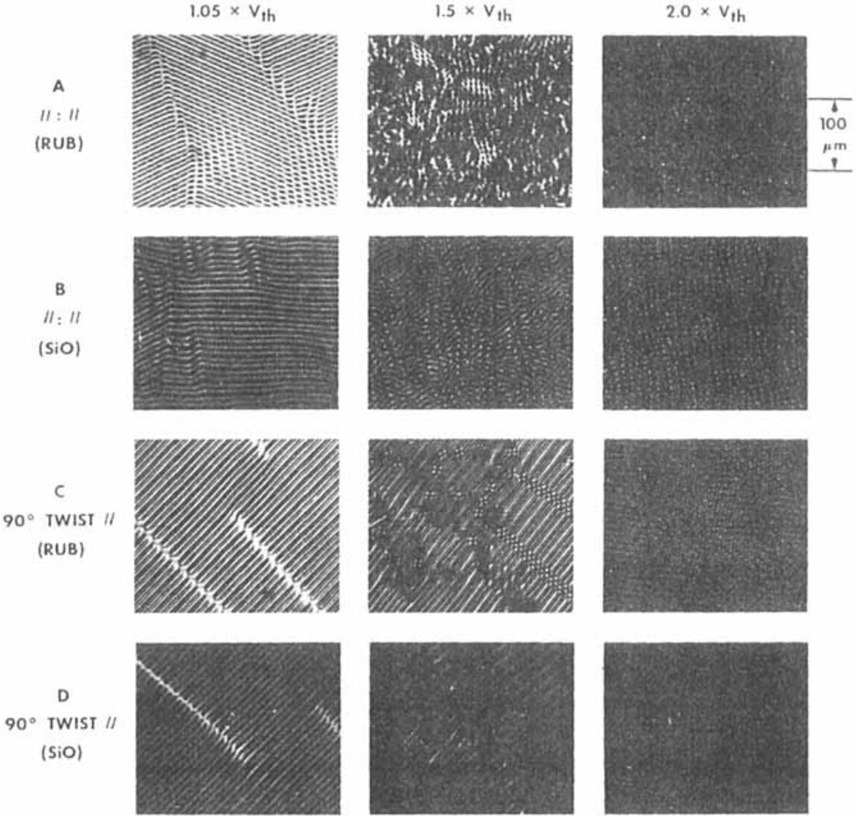

FIGURE 6 *(continued on facing page)*

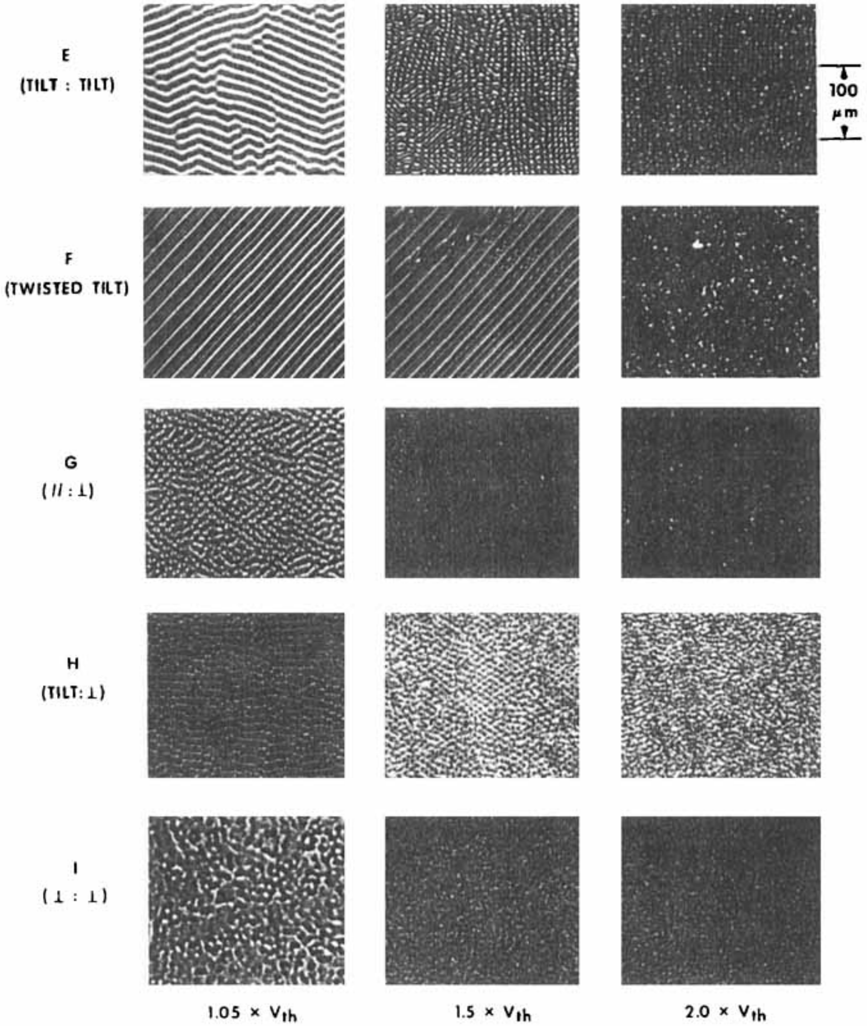

FIGURE 6 Microscopic pictures of dynamic scattering patterns with various alignment modes. Dopant: 0.1% TBATMS. (View is normal to electrode surfaces, with incident light polarized parallel to the surface-parallel alignment direction.)

without a twisted configuration. However, much longer decay times are shown for all other configurations in which $\bar{\theta} > 0$ ($\bar{\theta}$ between 36° and 90° for cells E, F, G, H, and I). This is in agreement with previous observations[30] that dynamic scattering from short pulses decayed faster in cells with surface-parallel compared to surface-perpendicular alignment. The delay and rise times are considerably longer when $\bar{\theta} = 90°$ than for other alignments, and there appears to be some increase in delay and rise times in the $\bar{\theta} = 36°$ to $63°$ range as compared to $\bar{\theta} = 0°$. These delay and rise time effects are probably related to the fact that with a fixed applied signal of 30 V the $V_{\text{applied}}/V_{\text{th}}$ ratio decreases as $\bar{\theta}$ increases. Alignment configuration F (twisted tilted) shows somewhat anomalous results of slow response times compared to the simple tilted alignment (E), although both F and E have $\bar{\theta} = 36°$ and have the same average V_{th} values.

Microscopic flow patterns

Microscope pictures of domains and dynamic scattering are shown in Figure 6, with comparisons for the nine alignments at the same $V_{\text{applied}}/V_{\text{th}}$ ratios with the TBATMS-doped liquid crystal. The pictures are taken with polarized light parallel to the parallel alignment direction on the incident electrode. Similar results are observed (but not shown) for the same liquid crystal doped with the DBF/TFM mixture. At low voltages the hydrodynamic flow patterns correspond to Williams-type[31] domains. The domain patterns for parallel[32] and twisted parallel[33] alignments have been observed previously. Each alignment shows a characteristic type of low voltage pattern. The twisted nematic alignments (C, D, and F) show the most regular patterns, which persist at higher V/V_{th} values than patterns with other alignments. The persistence of these fairly regular domain patterns instead of a more random turbulence may be related to the lower levels of scattering in the C, D, and F cells compared to other alignments in the $2V_{\text{th}}$ to $4V_{\text{th}}$ range, as shown in Figures 2 and 3. The splay (G, H) and particularly the perpendicular alignment (I) show the least regular patterns and they go into random turbulence at lower V/V_{th} values. The surface-perpendicular cells appear to have virtually no regular domain patterns just slightly above V_{th}.

Acknowledgment

We are indebted to the Directorate of Chemical Sciences, Air Force Office of Scientific Research, Contract F44620-72-C-0075 for partial financial support of this research.

References

1. G. H. Heilmeier, L. A. Zanoni, and L. A. Barton, *Appl. Phys. Lett.*, **13**, 46 (1968).
2. J. D. Margerum and L. J. Miller, *J. Colloid and Interface Science*, a review article, in press.
3. G. H. Heilmeier, L. A. Zanoni, and L. A. Barton, *Proc. IEEE*, **56**, 1162 (1968).
4. G. H. Heilmeier, L. A. Zanoni, and L. A. Barton, *IEEE Trans. Electron Devices*, **ED-17**, 22 (1970).
5. P. G. de Gennes, *Comments Solid State Phys.*, **3**, 35 (1971).
6. H. Koelmans and A. M. van Boxtel, *Mol. Cryst. Liq. Cryst.*, **12**, 185 (1971); *Phys. Lett.*, **32A**, 32 (1970).

7. S. Matsumoto, M. Kawamoto, and T. Tsukada, *Chem. Lett.*, **1973**, 837.
8. R. E. Aldrich and R. B. Lauer, *IEEE Conference Records of 1972 Conference on Display Devices*, October 11–12, 1972.
9. J. D. Margerum, H. S. Lim, P. O. Braatz, and A. M. Lackner, *6th International Liq. Cryst. Conf., Kent, Ohio*, August 1972, Paper K-1, *Mol. Cryst. Liq. Cryst.*, **38**, 219 (1977).
10. F. E. Wargocki and A. E. Lord, Jr., *J. Appl. Phys.*, **44**, 831 (1973).
11. G. Elliott, E. Harvey, and M. G. Williams, *Electronics Lett.*, **9**, 399 (1973).
12. H. S. Lim and J. D. Margerum, *J. Electrochem. Soc.*, **123**, 837 (1976).
13. H. S. Lim and J. D. Margerum, *Appl. Phys. Lett.*, **28**, 378 (1976).
14. A. I. Baise, I. Teucher, and M. M. Labes, *Appl. Phys. Lett.*, **21**, 142 (1972).
15. L. T. Creagh and A. R. Kmetz, *J. Electron. Mat.*, **1**, 350 (1972).
16. L. T. Creagh, A. R. Kmetz, and R. A. Reynolds, *IEEE Trans. Electron Devices*, **ED-18**, 672 (1971).
17. W. Helfrich, *J. Chem. Phys.*, **51**, 4092 (1969).
18. H. Gruler, *Mol. Cryst. Liq. Cryst.*, **27**, 31 (1974).
19. P. A. Penz and G. W. Ford, (a) *Phys. Review A*, **6**, 414 (1973); (b) *Phys. Review A*, **6**, 1676 (1972).
20. K. Ronseau, G. C. Farrington, and D. Dolphin, *J. Org. Chem.*, **37**, 3968 (1972).
21. E. Guyon, P. Pieranski, and M. Boix, *Lett. Appl. Eng. Sci.*, **1**, 19 (1973).
22. J. L. Janning, *Appl. Phys. Lett.*, **21**, 173 (1972).
23. D. Myerhofer, *J. Appl. Phys.*, **46**, 5084 (1975).
24. M. F. Schiekel and K. Fahrenschon, *Appl. Phys. Lett.*, **19**, 391 (1971).
25. M. Ohtsu, T. Akahne, and T. Tako, *Japan J. Appl. Phys.*, **13**, 621 (1974).
26. A. E. Baise and M. M. Labes, *J. Chem. Phys.*, **59**, 551 (1973).
27. P. A. Penz, *Mol. Cryst. Liq. Cryst.*, **23**, 1 (1973).
28. E. Dubois-Violetti, *et al.*, *Phys. Rev. Lett.*, **25**, 1642 (1970).
29. M. I. Barnik, L. M. Blinov, M. F. Grabenkin, S. A. Pikin, and V. G. Chigrinov, *Zh. Eksp. Teor. Fiz.*, **69**, 1080 (1975).
30. S. Aftergut and H. S. Cole, *1972 SID International Symposium Digest of Technical Papers*, June 1972, San Francisco, Calif., p. 92.
31. R. Williams, *J. Chem. Phys.*, **39**, 384 (1963).
32. W. Helfrich, *Mol. Cryst. Liq. Cryst.*, **21**, 187 (1973).
33. J. J. Wright and J. F. Dawson, *Phys. Lett.*, **43A**, 145 (1973).